High-frequency interaction-induced rototranslational scattering from gaseous nitrogen

T. Bancewicz
Nonlinear Optics Division, Institute of Physics, Adam Mickiewicz University, Grunwaldzka 6, 60-780 Poznań, Poland

V. Teboul and Y. Le Duff
Laboratoire des Propriétés Optiques des Matériaux et Applications, Université d'Angers, Faculté des Sciences, 2 boulevard Lavoisier, 49045 Angers, France

(Received 9 September 1991; revised manuscript received 24 March 1992)

N_2 gas rototranslational scattering is studied at high frequency up to 700 cm^{-1} theoretically and experimentally for several temperatures and from low densities up to 170 amagat. Our theoretical calculations take into account multipole contributions from the mean value and anisotropy of the dipole-dipole polarizability tensor $\overleftrightarrow{a}$ and two independent components of the dipole-octopole polarizability tensor $\overleftrightarrow{E}$. The $\overleftrightarrow{E}$ tensor is found to give the most important contribution at high frequency. The comparison of the experimental and theoretical spectra allows us to estimate at $|\bar{E}_0^{(4)}|=4.6$ Å^5 the absolute value of the experimental ($\lambda=514.5$ nm) dynamic irreducible spherical component of the dipole-octopole polarizability tensor of N_2. When using this value, good agreement is obtained between the theoretical and experimental spectra at room temperature (294 K) and low temperature (150 K).

PACS number(s): 34.50.−s, 33.20.Fb, 33.70.−w

I. INTRODUCTION

Light scattering has been widely used in recent years to study molecular interactions in fluids [1–4]. It has been shown for atomic fluids [3,5] and for several optically isotropic molecular fluids [2,4,6(a),6(b)] that dipole-induced dipole (DID) interactions explain most of the integrated induced intensities as well as the low-frequency part of the interaction-induced spectra. However, when higher-frequency scattering is considered, shorter-range mechanisms are necessary to explain the observed interaction-induced scattering (IIS). The interaction-induced dipole moment for the molecule of a fluid illuminated by an incident laser field has to involve its molecular dipole-multipole polarizabilities. If μ is the dipole induced by a local field $\mathcal{E}$, neglecting hyperpolarizabilities we have [7]

$$\mu_\alpha = a_{\alpha\beta}\mathcal{E}_\beta + \tfrac{1}{3}A_{\alpha\beta\gamma}\mathcal{E}_{\beta\gamma} + \tfrac{1}{15}E_{\alpha\beta\gamma\delta}\mathcal{E}_{\beta\gamma\delta} + \cdots , \quad (1)$$

where $\overleftrightarrow{a}$, $\overleftrightarrow{A}$, $\overleftrightarrow{E}$ are dipole-multipole polarizability tensors of the molecule. The multipoles involved are, respectively, the dipole-, the quadrupole-, and the octopole-induced moments. The subscripts α, β, γ, and δ refer to Cartesian axes. $\mathcal{E}_{\beta\gamma}$ and $\mathcal{E}_{\beta\gamma\delta}$ are the $\beta\gamma$ and $\beta\gamma\delta$ components of the local-field gradients acting on the molecule. For tetrahedral and octrahedral molecules [CH_4,CF_4,$C(CH_3)_4$,SF_6] it has been shown [6(a),7–10] that the polarizability tensors $\overleftrightarrow{A}$ and/or $\overleftrightarrow{E}$ contribute to the far-frequency wings.

For linear centrosymmetric molecules, the dipole-quadrupole polarizability tensor vanishes, and the next multipolar contribution after the dipole-dipole contribution comes from the dipole-octopole polarizability $\overleftrightarrow{E}$. For these centrosymmetric molecules the $\overleftrightarrow{E}$ tensor has two independent components [11,12], contrary to the already investigated molecules belonging to the symmetry groups T_d or O_h for which $\overleftrightarrow{E}$ has only one independent component. Furthermore, if the molecules are optically anisotropic, the rototranslational scattering includes a depolarized contribution from the anisotropy of the intrinsic polarizability [13], which generally is mixed with interaction-induced intensities [14–21].

The present work is a study, both theoretical and experimental, of the spectral shape of far rototranslational scattering from the linear centrosymmetric molecule N_2 up to frequency shifts of about 700 cm^{-1}, where the scattered intensities are purely interaction induced. Since the radial dependencies of the induced mechanisms described by the terms of Eq. (1) due, respectively, to the $\overleftrightarrow{a}$ tensor (DID) and $\overleftrightarrow{E}$ tensor (DIO), are significantly different, one may expect quite different spectral shapes for these mechanisms. Thus, in our work we found good conditions for the observation of short-range contributions to IIS and particularly the contribution from the dipole-octopole polarizability tensor $\overleftrightarrow{E}$. In our study, several densities and temperature conditions have been considered.

Our paper is organized as follows. In Sec. II we give the multipolar theory of the spectral shape of scattered light, devoting special attention to different broadening procedures of the rotational stick spectrum due to translational motions of the N_2 molecules. Section III describes the experimental setup and procedures used, whereas in Sec. IV we compare the theoretically calculated spectra with those obtained experimentally.

II. THEORY

A. General considerations

We consider a system composed of a large number N of like, intrinsically anisotropic molecules on which monochromatic laser radiation of frequency ω_i linearly polarized in the direction **e** is incident. The radiation scattered at ω_s is measured on traversal of an analyzer with

polarization **n**. Theoretically, the polarized (**e**∥**n**) and depolarized (**e**⊥**n**) double-differential scattering cross sections are expressed by [3,10]

$$\frac{\partial^2\sigma}{\partial\Omega\partial\omega}=k_i k_s^3\frac{1}{2\pi}\int \exp(-i\omega t)F(t)dt \ , \tag{2}$$

where

$$F(t)=\sum_{l=0,2}\phi_{ll}^0 F_{ll}^0(t) \ , \tag{2a}$$

with

$$\phi_{00}^0=\tfrac{1}{3}(\mathbf{e}\cdot\mathbf{n})^2 \ , \tag{2b}$$

$$\phi_{22}^0=\tfrac{1}{30}[3+(\mathbf{e}\cdot\mathbf{n})^2] \ . \tag{2c}$$

$F_{ll}^0(t)$ is the autocorrelation function

$$F_{ll}^0(t)=\langle \overleftrightarrow{\Pi}^{(l)}(0)\odot\overleftrightarrow{\Pi}^{(l)}(t)\rangle \tag{3}$$

of the irreducible lth rank pair polarizability tensor $\Pi^{(l)}$ of the scattering molecules. In Eq. (2), $\odot$ denotes a scalar tensor product and $\langle\ \rangle$ is a canonical average. Here, since we discuss the depolarized VH scattering, we are dealing with the following cross section:

$$\frac{\partial^2\sigma_{\mathrm{VH}}}{\partial\Omega\partial\omega}=\frac{k_i k_s^3}{10}\frac{1}{2\pi}\int \exp(-i\omega t)F_{22}^0(t)dt \ . \tag{2'}$$

When considering intermolecular interactions, the pair polarizability $\overleftrightarrow{\Pi}^{(l)}$ may be separated into two parts:

$$\overleftrightarrow{\Pi}^{(l)}={}_{(M)}\overleftrightarrow{\Pi}^{(l)}+{}_{(\mathrm{DIM})}\overleftrightarrow{\Pi}^{(l)} \ , \tag{4}$$

the overall intrinsic molecular polarizability ${}_{(M)}\overleftrightarrow{\Pi}^{(l)}$ of the pair, and the polarizability ${}_{(\mathrm{DIM})}\overleftrightarrow{\Pi}^{(l)}$, originating in the interaction-induced dipole-induced multipole mechanisms. In a first-order approximation, the excess ${}_{(\mathrm{DIM})}\overleftrightarrow{\Pi}^{(l)}$ polarizability is expressed in terms of the multipole series expansion [22]

$${}^{(1)}_{(\mathrm{DIM})}\overleftrightarrow{\Pi}^{(l)}={}^{(l)}_{(\mathrm{DID})}\overleftrightarrow{\Pi}^{(l)}+{}^{(l)}_{\mathrm{DIQ})}\overleftrightarrow{\Pi}^{(l)}+{}^{(l)}_{(\mathrm{DIO})}\overleftrightarrow{\Pi}^{(l)} \ , \tag{5}$$

where the first term is the dipole-induced dipole contribution well known from the Yvon-Kirkwood theory and the second and third terms represent, respectively, the dipole-induced quadrupole (DIQ) and dipole-induced octopole contributions.

The theory of the irreducible spherical representation of the dipole-induced multipole pair polarizability has been developed by us elsewhere [23]. Here, we give only the final result for the β component of the irreducible Jth-rank pair-polarizability tensor ${}^{(1)}_{(\mathrm{DIM})}\overleftrightarrow{\Pi}_{J\beta}$ in the coupling scheme most convenient for our present calculations:

$${}^{(1)}_{(\mathrm{DIM})}\overleftrightarrow{\Pi}_{J\beta}=\sum_{\substack{p,q=1,2\\(p\neq q)}}\sum_{\substack{J_1,J_2,J_3\\l_1,l_2,N}}(-)^{J_1+N}\left[\frac{2^N}{(2l_1)!(2l_2)!}\right]^{1/2}X_{J_1J_2J_3N}\begin{Bmatrix}J_1&J_2&J_3\\1&1&J\\l_1&l_2&N\end{Bmatrix}\{\overleftrightarrow{\mathbf{T}}_N(pq)\otimes[\overleftrightarrow{\mathbf{A}}_{J_1}^{(1l_1)}(p)\otimes\overleftrightarrow{\mathbf{A}}_{J_2}^{(1l_2)}(q)]_{J_3}\}_{J\beta} \ , \tag{6}$$

where

$$\begin{Bmatrix}a&b&c\\d&e&f\\g&h&j\end{Bmatrix}$$

is the 9-j Wigner symbol, $\overleftrightarrow{\mathbf{A}}_j^{(1l)}(r)$ is the irreducible Jth-rank spherical tensor of multipole polarizability of molecule r, and $\overleftrightarrow{\mathbf{T}}_N$ denotes the spherical multipole interaction tensor. Moreover $X_{a,b,\ldots f}=[(2a+1)(2b+1)\ldots(2f+1)]^{1/2}$, $l_1+l_2=N$, and $\otimes$ stands for an irreducible tensor product.

We shall consider here gaseous nitrogen at low density. In this case, the rotational and translational molecular motions are treated separately. In this approximation the cross contributions to the scattered intensity between different terms of (5) vanish. Moreover, due to the center of symmetry of the nitrogen molecule, the first-order DIQ contribution of (5) vanishes, too. In this way the intensity of scattered radiation is composed by three quadratic terms [23]: intrinsic, DID, and DIO.

For linear molecules, the rotational Rayleigh cross section due to permanent intrinsic anisotropy has the well-known form [24]

$$\frac{\partial^2\sigma_{\mathrm{VH}}}{\partial\Omega\partial\omega}=\frac{1}{10}\frac{\exp(-E_J/k_BT)}{Z}g_I(2J+1)(2J'+1)\times\begin{bmatrix}J'&2&J\\0&0&0\end{bmatrix}^2\left|\tilde{A}_{20}^{(11)}\right|^2\delta(\omega-\Delta\omega) \ , \tag{7}$$

where

$$\begin{bmatrix}a&b&c\\0&0&0\end{bmatrix}$$

is the 3-j Wigner symbol, $E_j=BJ(J+1)$ denotes the energy of the rotational levels of the N_2 molecule, g_I denotes the nuclear statistical factor, and Z is the rotational partition function. $\tilde{A}_{20}^{(11)}$ is the 0th component of the irreducible second-rank dipole-dipole polarizability tensor in the molecular frame and $\delta(x)$ stands for the Dirac δ function.

To deal with contributions to the scattered intensity resulting from interaction-induced mechanisms, we have to calculate the autocorrelation function of (6). Using the decoupling procedure for the spherical irreducible tensors $\overleftrightarrow{\mathbf{A}}$, $\overleftrightarrow{\mathbf{B}}$, $\overleftrightarrow{\mathbf{C}}$, and $\overleftrightarrow{\mathbf{D}}$ [25],

$$[(\vec{\vec{A}}^{(a)}\otimes\vec{\vec{B}}^{(b)})^{(c)}]\odot[(\vec{\vec{D}}^{(d)}\otimes\vec{\vec{E}}^{(e)})^{(c)}]$$
$$=(-)^{2a+b-d}\sum_g X_c^2\begin{Bmatrix}a & b & c\\ e & d & g\end{Bmatrix}[(\vec{\vec{A}}^{(a)}\otimes\vec{\vec{D}}^{(d)})^{(g)}]$$
$$\odot[(\vec{\vec{B}}^{(b)}\otimes\vec{\vec{E}}^{(e)})^{(g)}]\ , \tag{8}$$

with

$$\begin{Bmatrix}a & b & c\\ e & d & g\end{Bmatrix}$$

denoting the 6-j Wigner symbol, we can easily separate the translational and rotational degrees of freedom in our autocorrelation function. Since, for an isotropic fluid, the mean values occurring in Eq. (3), the rotational and translational parts of our correlation function, have to be rotational invariants [26], in our autocorrelation function only the terms with $g=0$ differ from zero. General results for the dipole-induced multipole rotational and translational correlation functions as well as the procedure leading to the rotational stick spectrum have been given elsewhere [27]. We calculate our stick spectrum assuming that the molecules of the scattering volume rotate freely in accordance with the predictions of quantum mechanics [7,27]. In Ref. [27] we have used first-order information theory to broaden our stick spectra. Here we additionally use more-sophisticated broadening translational spectra resulting from Mori's theory [28] as well as from the Birnbaum-Cohen theory [29].

B. Broadening functions

To apply Mori as well as Birnbaum-Cohen theory for broadening our stick spectra, we have to calculate the second ($l=2$) and fourth ($l=4$) moments $M_l^{(N)}$ of the translational part

$$^{\mathrm{tr}}C^{(N)}(t)=\langle\vec{\vec{T}}^{(N)}(\mathbf{r}_{12}(0))\odot\vec{\vec{T}}^{(N)}(\mathbf{r}_{12}(t))\rangle \tag{9}$$

of our dipole-induced dipole ($N=2$) and dipole-induced octopole ($N=4$) correlation functions, and normalize them to their zero moments ($\hat{M}_l^{(N)}=M_l^{(N)}/M_0^{(N)}$).

To calculate the moments, we follow the procedure developed in [30]. The zeroth DID and DIO translational moments read

$$M_0^{(2)}=6\langle r_{12}^{-6}\rangle\ , \tag{10a}$$

$$M_0^{(4)}=2520\langle r_{12}^{-10}\rangle\ , \tag{10b}$$

whereas the normalized second moments of, respectively, the DID and DIO mechanisms have the forms

$$\hat{M}_2^{(2)}=15(\beta m_{12})^{-1}\langle r_{12}^{-8}\rangle/\langle r_{12}^{-6}\rangle\ , \tag{11a}$$

$$\hat{M}_2^{(4)}=45(\beta m_{12})^{-1}\langle r_{12}^{-12}\rangle/\langle r_{12}^{-10}\rangle\ . \tag{11b}$$

Then, assuming a spherical potential between nitrogen molecules, for the normalized fourth moments we obtain

$$\hat{M}_4^{(2)}=3(\beta m_{12})^{-2}\frac{\langle 280r_{12}^{-10}+3[\beta U'(r_{12})]^2r_{12}^{-8}\rangle}{\langle r_{12}^{-6}\rangle}\ , \tag{12a}$$

$$\hat{M}_4^{(4)}=5(\beta m_{12})^{-2}\frac{\langle 1188r_{12}^{-14}+5[\beta U'(r_{12})]^2r_{12}^{-12}\rangle}{\langle r_{12}^{-10}\rangle}\ , \tag{12b}$$

where $\beta=1/k_BT$, m_{12} is the reduced molecular mass (for nitrogen, $m_{12}=2.326\times10^{-26}$ kg), and $\langle\ \rangle$ denotes the low-density mean value of $F(r_{12})$:

$$\langle F(r_{12})\rangle=\int\int\int F(r_{12})\exp[-\beta U(r_{12})]d\Omega_1d\Omega_2d\mathbf{r}_{12}\Big/\int\int d\Omega_1d\Omega_2\ , \tag{13}$$

where $U(r_{12})$ stands for the intermolecular potential of nitrogen molecules and $U'(r_{12})=[dU(r_{12})]/dr_{12}$.

Since the assumptions leading to Eqs. (10)–(12) require a spherical, or nearly spherical, nitrogen potential, we calculate the mean values occurring in Eqs. (10)–(12) using the isotropic part of the spherical-harmonic expansion of the modern N_2 potential recently proposed by Ling and Rigby [31(a)] and van der Avoird, Worner, and Jansen [31(b)]:

$$U(r_{12})=U_{\mathrm{overlap}}^{0,0,0}(r_{12})+U_{\mathrm{disp}}^{0,0,0}(r_{12})\ , \tag{14a}$$

where

$$U_{\mathrm{overlap}}^{0,0,0}(r_{12})=F^{0,0,0}=\exp(-\alpha^{0,0,0}r_{12}-\beta^{0,0,0}r_{12}^2)\ , \tag{14b}$$

$$U_{\mathrm{disp}}^{0,0,0}(r_{12})=-\sum_{n=6,8,10}f_n^{0,0,0}(r_{12})C_n^{0,0,0}r_{12}^{-n}\ , \tag{14c}$$

with $f_n^{0,0,0}(r_{12})$ denoting damping functions of [31(b)]. The respective parameters of (14) used in our calculations are [31(b)] $F^{0,0,0}=7.080\times10^{-9}$ erg, $\alpha^{0,0,0}=2.64733$ Å^{-1}, $\beta^{0,0,0}=0.12978$ Å^{-2}, $C_6^{0,0,0}=6.840\times10^{-11}$ erg Å^6, $C_8^{0,0,0}=6.302\times10^{-10}$ erg Å^8, $C_{10}^{0,0,0}=5.797\times10^{-9}$ erg Å^{10}.

The numerical values of the DID and DIO translational zeroth, second, and fourth moments for the two temperatures 294 and 150 K considered here are assembled in Table I, where we moreover give for comparison the appropriate values computed with the Lennard-Jones nitrogen potential

$$U(r_{12})=4\varepsilon[(\sigma/r_{12})^{12}-(\sigma/r_{12})^6]\ , \tag{15}$$

where [32] $\varepsilon/k_B=91.5$ K and $\sigma=3.681$ Å.

Having calculated the normalized second and fourth translational moments and using a Gaussian form for the first-order memory function, which, by information theory, is predicted as the least-biased choice we can make with the available knowledge concerning the system [30], Mori theory gives us the translational spectrum in the form [33,34]

$$I_{\mathrm{tr}}^{(N)}(\omega)=\frac{M_0^{(N)}}{\pi}\frac{R(\omega)}{R^2(\omega)+[\omega+S(\omega)]^2}\ , \tag{16}$$

TABLE I. The theoretical DID and DIO translational moments for two temperatures and two types of potential. The first two rows assemble the DID and DIO zeroth moments. The next four rows give the second M_2 and fourth M_4 DID and DIO moments normalized to their respective zeroth moments M_0.

Moments \ Temperature	Mechanism	Modern [31] potential 294 K	Modern [31] potential 150 K	Lennard-Jones [32] potential 294 K	Lennard-Jones [32] potential 150 K
$M_0^{(2)}$ (Å^{-3})	DID	0.603	0.648	0.700	0.778
$M_0^{(4)}$ (Å^{-7})	DIO	0.676	0.674	0.899	0.929
$(M_2^{(2)}/M_0^{(2)})$ (units of 10^{26}s^{-2})	DID	0.125	0.062	0.134	0.066
$(M_2^{(4)}/M_0^{(4)})$ (units of 10^{26}s^{-2})	DIO	0.477	0.229	0.511	0.246
$(M_4^{(2)}/M_0^{(2)})$ (units of 10^{52}s^{-4})	DID	0.188	0.050	0.217	0.058
$(M_4^{(4)}/M_0^{(4)})$ (units of 10^{52}s^{-4})	DIO	1.56	0.381	1.81	0.439

where

$$R(\omega)=\sqrt{\pi/2}\frac{\Delta_1}{\sqrt{\Delta_2}}\exp\left[-\frac{\omega^2}{2\Delta_2}\right], \tag{16a}$$

$$S(\omega)=-\frac{\sqrt{2}\Delta_1}{\Delta_2}\exp\left[-\frac{\omega^2}{2\Delta_2}\right]\int_0^{\omega/(2\Delta_2)^{1/2}}\exp(z^2)dz , \tag{16b}$$

with $\Delta_1=\hat{M}_2$ and $\Delta_2=\hat{M}_4/\hat{M}_2-\hat{M}_2$.

Using the values of Table I, we calculate Δ_1 and Δ_2 for the DID and DIO mechanisms, respectively, and by means of Eq. (16) we broaden our stick DID and DIO spectra using Mori theory. The Birnbaum-Cohen model requires, moreover, knowledge of the normalized second and fourth spectral moments. Then the model spectral shape reads [29]

$$I_{\mathrm{BC}}^{(N)}(\omega)=\frac{M_0^{(N)}\tau_1}{\pi}\exp(\tau_2/\tau_1)\exp(\omega\tau_0)\frac{zK_1(z)}{1+(\omega\tau_1)^2} , \tag{17}$$

with the parameters defined as

$$\tau_0=\frac{\hbar}{2k_BT} , \tag{18a}$$

$$\tau_1=(\hat{M}_2)^{-1/2}\left[\frac{\hat{M}_4}{3\hat{M}_2^2}-1\right]^{1/2} , \tag{18b}$$

$$\tau_2=(\hat{M}_2)^{-1/2}\left[\frac{\hat{M}_4}{3\hat{M}_2^2}-1\right]^{-1/2} , \tag{18c}$$

$$z=\frac{[1+(\omega\tau_1)^2]^{1/2}(\tau_2^2+\tau_0^2)^{1/2}}{\tau_1} , \tag{18d}$$

and $K_l(z)$ is a modified Bessel function of the second kind. This function may be approximated by [35]

$$K_1(x)=1.01[\exp(-x)/x](1+1.69x)^{1/2} , \tag{19}$$

with a maximum error of 1%. Using Eqs. (18), (19), and the values of Table I, we broaden our stick DID and DIO spectra with the Birnbaum-Cohen model function (17). Studying the values of Table I, we conclude that in all cases the modern nitrogen potential predicts lower values of the respective moments by comparison with the values resulting from the center-center Lennard-Jones potential. Moreover, from this table we note that for both types of potential considered, the zeroth moments differ in their values more significantly than the respective normalized moments. This suggests that small differences between the normalized second and fourth moments calculated for the modern and Lennard-Jones potential are, to a large extent, due to the fortunate cancellation upon normalization of more significant differences in the unnormalized moments. For this reason and due to the feature of the rototranslational spectrum given in Ref. [8] showing that the rototranslational far wing is, in fact, slightly sensitive to the details of the broadening function and essentially reflects the distribution of the individual rotational lines of the stick spectrum, we find that the shape of our spectra is not very sensitive to the difference between the two potentials used in the calculations. Due to the difference between the zeroth moments, the choice of potential has, however, a more pronounced influence on the absolute intensity. In the figures we present our spectra resulting from the modern potential.

For each broadening procedure we have calculated the absolute differential scattering cross section of our DID and DIO theoretical spectra, integrating them over frequency by Simpson's method and comparing the numerical values with those calculated from the analytical formulas obtained by us [23] previously:

$$V\left[\frac{\partial\sigma_{\mathrm{VH}}}{\partial\Omega}\right]_{\mathrm{DID}}=k_s^3k_i[\tfrac{2}{15}(\tilde{A}_{00}^{(11)})^4+\tfrac{7}{75}(\tilde{A}_{20}^{(11)}\tilde{A}_{20}^{(11)})^2+\tfrac{11}{125}(\tilde{A}_{20}^{(11)})^4]\langle r_{12}^{-6}\rangle , \tag{20a}$$

$$V\left[\frac{\partial\sigma_{\mathrm{VH}}}{\partial\Omega}\right]_{\mathrm{DIO}}=k_s^3k_i/90[\tfrac{8}{15}(\tilde{A}_{00}^{(11)}\tilde{A}_{20}^{(13)})^2+\tfrac{18}{75}(\tilde{A}_{20}^{(11)}\tilde{A}_{20}^{(13)})^2+\tfrac{154}{405}(\tilde{A}_{20}^{(11)}\tilde{A}_{40}^{(13)})^2+\tfrac{11}{81}(\tilde{A}_{00}^{(11)}\tilde{A}_{40}^{(13)})^2]\langle r_{12}^{-10}\rangle , \tag{20b}$$

where V is the active scattering volume. The above two sets of values were always in quite good agreement, differing by less than several percent.

III. EXPERIMENT

We measured the light scattering of gaseous N_2 using a 90°-scattering experiment. The beam of an argon-ion laser operating on the 514.5-nm line with 2 W of power was focused in a four-window cell containing the sample. Different types of cells were used for this work. For low temperature we used a high-pressure cell especially built to fit with a helium continuous-flow cryostat. The temperature was controlled inside the cell by a calibrated platine resistor. The accuracy of the sample temperature was estimated at about 0.5 K. The sample cells were designed specially in order to minimize the parasitic light due to internal reflexions. This was obtained by using antireflecting coating on the cell windows and blackened diaphragms on the laser and the scattering beams. The light scattered at 90° was analyzed with a U 1000 Jobin-Yvon double monochromator designed to optimize its luminosity. Finally, the signal was detected by a low-dark-noise cooled EMI 9789A photomultiplier. The whole experiment was controlled automatically by means of a computer. For each wavelength, several measurements were made and analyzed according to statistical tests. When the data were found to be satisfying, the grating of the monochromator was shifted to another wavelength.

Several polarization conditions were studied by changing the polarization of the laser field. Using a half-wave plate associated with a Glan polarizer, we were able to study the spectra $I_V(\omega)$ and $I_H(\omega)$, where V and H indicate the laser polarization in directions perpendicular or parallel to the scattering plane [36], respectively. $I_V(\omega)$ and $I_H(\omega)$ represent the observed intensities. Due to the finite value of the scattering collection angle, the 90° scattering anisotropic spectrum [37] $I_{\rm ani}(\omega)$ proportional to the Fourier transform of the correlation function of the polarizability anisotropy β is generally a linear function of the observed quantities $I_H(\omega)$ and $I_V(\omega)$. We have [38,39]

$$I_{\rm ani}(\omega)=\tfrac{1}{2}[aI_H(\omega)+bI_V(\omega)] , \tag{21}$$

where a and b are constants. For room temperature, the maximum of the scattering angle θ used was 6.2° and we had $a=1.006$ and $b=-0.006$. For low temperature, the maximum of the scattering angle was smaller and we used

$$I_{\rm ani}(\omega)=\tfrac{1}{2}I_H(\omega) . \tag{22}$$

In our experiment some contribution to the scattering intensities has been observed from dust inside the cell. We reduced this effect by waiting several hours after each change of the gas density inside the cell. The cell was filled through a dust filter (4 μm). Nitrogen, containing less than 1 ppmV (part per million by volume) of impurities was purchased from UCAR. We used PVT data given in Ref. [40].

IV. RESULTS AND DISCUSSION

We have studied rototranslational scattering from gaseous N_2 at several densities up to 170 amagat. The Stokes scattering intensities have been measured by us for frequency shifts up to 700 cm^{-1} with quite large slits for the double monochromator. Our apparatus function for the far wings was about 8 cm^{-1} (full width at half maximum). Two temperatures were used for N_2: 294 and 150 K. For room temperature, the density dependence of the intensities was studied for several frequency shifts. We show in Fig. 1, for increasing densities, the scattering intensity $I(450)$ measured for a frequency shift of $\nu=450$ cm^{-1} relative to the intensity $I(60)$ measured for $\nu=60$ cm^{-1} at the same density. The ratio $I(450)/I(60)$ increases linearly with density up to 170 amagat. From those results and assuming that the intensity measured at $\nu=60$ cm^{-1} was predominantly due to permanent polarizability anisotropy and proportional to the gas density and the local field, it follows that the scattering in the high-frequency part of the N_2 Rayleigh spectra is induced by binary mechanisms.

We have calculated the theoretical anisotropic spectra as the convolution of the rotational stick spectra and the above-described translational broadening spectra. We performed our calculations at room temperature (294 K) and two densities (41.5 and 170 amagat) and for low temperature (150 K) at 40.5 amagat. When dealing with the permanent anisotropy spectrum, we broadened the stick spectrum resulting from Eq. (7) with the Gaussian apparatus function having full width at a half maximum of 8 cm^{-1}. Figure 2 shows separately the theoretical intrinsic anisotropy as well as the DID and DIO contributions to the N_2 spectrum calculated for 41.5 amagat at 294 K. The importance of the DIO contribution to the resulting spectrum, especially at the far frequency of the spectrum, is clearly seen from this figure. In Fig. 3 we present the permanent anisotropy plus DID spectrum, the spectra resulting from permanent anisotropy plus DID plus DIO mechanisms, for two values of $|\tilde{E}_0^{(4)}|$, as well as the experimental spectrum for 41.5-amagat nitrogen at 294 K. In this figure, as well as in the other figures of this paper,

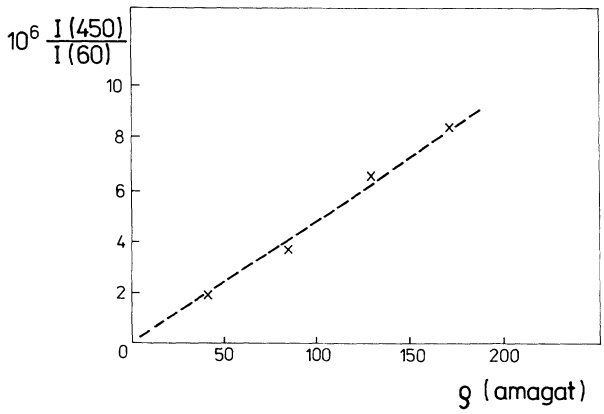

FIG. 1. Depolarized scattered intensity I_H (Stokes side) for frequency shift $\nu=450$ cm^{-1} divided by the depolarized scattered intensity for $\nu=60$ cm^{-1} measured at 294 K for N_2 gas vs density with a slit width of about 8 cm^{-1}.

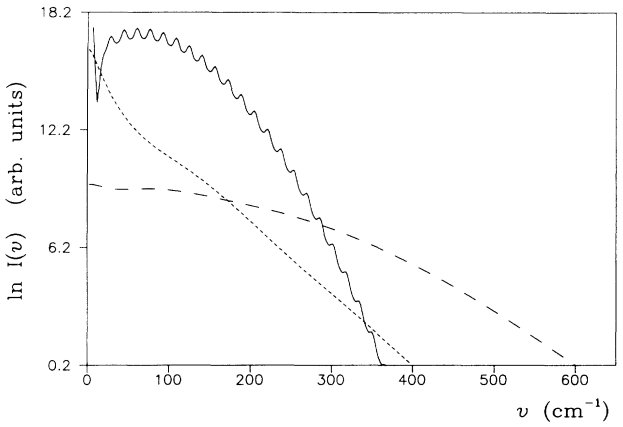

FIG. 2. Separate theoretical contributions to the anisotropic rototranslational spectrum of N_2 (Stokes side, 41.5 amagat, 294 K) due to permanent intrinsic anisotropy (——), the DID (----------), and DIO ($|\tilde{E}_0^{(4)}|=4.6$ Å^5) (— — —) light-scattering mechanisms.

the experimental anisotropic spectra have been adjusted to fit the theoretical depolarized intensity at frequency shift $\nu=60$ cm^{-1}. With this procedure, it is clearly seen from Fig. 3 that the DID mechanism alone is unable to describe the far-frequency part of the spectrum of gaseous nitrogen. Taking into account the DIO mechanism improves considerably the degree of agreement between the theoretical and experimental curves. In Cartesian coordinates the typical contribution to the pair polarizability due to the dipole-octopole mechanism reads

$$_{(\mathrm{DIO})}\Pi_{\alpha\beta}=\tfrac{1}{15}a_{\alpha\gamma}(1)T_{\gamma\delta\varepsilon\phi}(r_{12})E_{\delta,\varepsilon\phi\beta}(2)\ . \tag{23}$$

The numerical values of the dipole-dipole and dipole-octopole polarizability tensors used initially in our calculations are assembled in Table II. In spherical representation, the dipole-dipole polarizability tensor $a_{\alpha\gamma}$ decomposes into zero- and second-rank irreducible tensors, whereas the dipole-octopole polarizability tensor decomposes into irreducible tensors of rank 2 and 4. There are many rotational branches that are effective due to the DIO mechanism. From our numerical calculations we found, however, that the single rotational transition [7] DIO branch ($\Delta J_1=0$, $\Delta J_2=4$ or $\Delta J_1=4$, $\Delta J_2=0$) due to the spherical components $\tilde{A}_{00}^{(11)}=\tilde{\alpha}_0^{(0)}$ and $\tilde{A}_{40}^{(13)}=\tilde{E}_0^{(4)}$ has a decisive influence on the far-wing spectrum of N_2. However, the static $|\tilde{E}_0^{(4)}|=1.74$ Å^5 value resulting from numerical quantum-mechanical computations [42] gives us a too low intensity at the far wing of the spectrum in comparison with our experiment. To our knowledge there are as yet no numerical computations of the dynamic $E_{\alpha,\beta\gamma\delta}$ tensor of N_2, so we decided to estimate the value of $\tilde{E}_0^{(4)}$ from our experimental data. We obtain the best fit of the experimental and theoretical curves for the absolute value of $\tilde{E}_0^{(4)}$ equal to $|\tilde{E}_0^{(4)}|=4.6$ Å^5. We calculated spectra for other thermodynamical conditions using the above value for $\tilde{E}_0^{(4)}$. Applying different broadening functions for 294 K, we found no significant difference in the final spectrum using first-order information theory [27], Mori theory, or Birnbaum-Cohen model broadening. We thus conclude, in agreement with Ref. [8], that the profile of the rototranslational far wing is not sensitive to the details of the broadening function but reflects the distribution of the individual rotational lines of the stick spectrum. The situation is slightly different at low temperature, as we will show below. We have also studied the scattering at higher density. Figure 4 shows a comparison between the experimental and theoretical curves of the Stokes-side nitrogen spectrum at 294 K for 170 amagat. Since at this density the scattered signal was stronger, we were able to go further into the wing than previously. The DIO mechanism again reproduces very well the wing of the N_2 spectrum in the frequency range 300–500 cm.$^{-1}$ However, above this frequency range some excess intensity appears. We attribute this intensity to a shorter-range mechanism than DIO, such as an over-

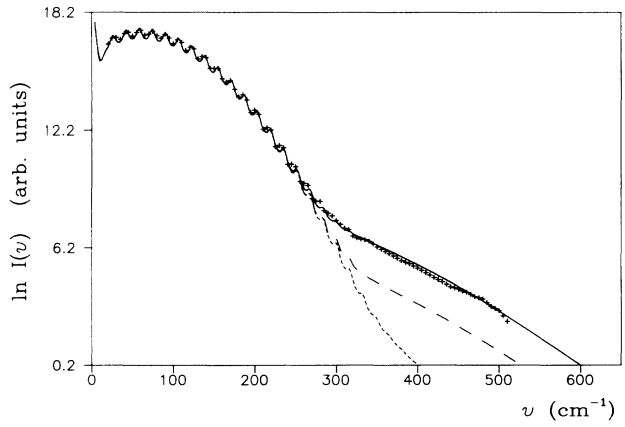

FIG. 3. Rototransitional anisotropic spectra of N_2 at 294 K and 41.5 amagat (Stokes side). Permanent anisotropy spectrum plus DID (----------); permanent anisotropy plus DID plus DIO ($|\tilde{E}_0^{(4)}|=1.74$ Å^5) spectrum (— — —); permanent anisotropy plus DID plus DIO ($|\tilde{E}_0^{(4)}|=4.6$ Å^5) spectrum (——) and experimental spectrum (+). In the course of our computations we noticed no significant influence of the value of the $\tilde{A}_{20}^{(13)}=\tilde{E}_0^{(2)}$ spherical component on the shape of the final theoretical spectrum. Due to the large slit function used (~8 cm^{-1}), the rotational structure from monomer motion is but slightly apparent in the experimental spectrum.

TABLE II. Numerical values of the dipole-dipole $\tilde{A}_{J0}^{(11)}$ and dipole-octopole $\tilde{A}_{J0}^{(13)}$ polarizability tensors used in our calculations.

J	$\tilde{A}_{J0}^{(11)}$ (Å^3)	$\tilde{A}_{J0}^{(13)}$ (Å^5)
0	−3.066[a]	
2	0.583[a]	0.609[b,c]
4		1.74[b,c]

[a]For $\lambda=514.5$ nm [41].

[b]Static (zero-frequency) value.

[c]We calculate the molecular-frame irreducible spherical components $\tilde{A}_{J0}^{(13)}$ of the dipole-octopole polarizability tensor used in our computations from the reducible spherical components $\tilde{\alpha}_{13m}$ computed in Ref. [42] using $\tilde{A}_{J0}^{(13)}=\sum_m(1m\ 3-m|J0)\tilde{\alpha}_{13m}$, where $(a\alpha\, b\beta|c\gamma)$ is the Clebsch-Gordan coefficient.

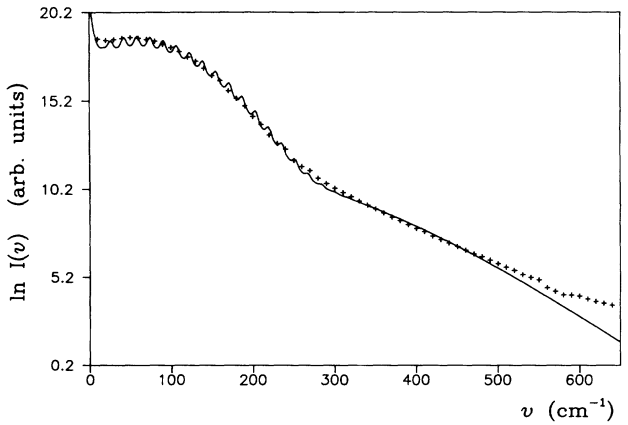

FIG. 4. Experimental (+) and theoretical (——) (permanent anisotropy plus DID plus DIO) anisotropic rotatranslational spectra of N_2 at 294 K and 170 amagat (Stokes side).

lap mechanism, or the next multipole polarizability of N_2. When modeling this contribution by an exponential curve $[\exp(-\nu/\nu_0)]$ with coefficient ν_0 equal to 450 cm^{-1} and on adding this contribution to the theoretical spectrum resulting from permanent anisotropy, DID, and DIO mechanisms, we obtain very good agreement with the experimental results, as shown in Fig. 5. Finally, in order to check the temperature dependence, we studied N_2 scattering at low temperature. Figure 6 shows a comparison between the theoretical and experimental results for the Stokes-side nitrogen spectrum at 150 K for 40.5 amagat. Since under these conditions the differences between the several models of broadening of the rotational stick spectrum are more strongly pronounced, we present and compare here the theoretical spectra obtained by different broadening procedures with the experimental spectrum. For the low temperature, all far-rototranslational theoretical spectra are generally slightly weaker than the experimental spectrum. From this figure one notes, however, that the Birnbaum-Cohen and Mori broadening procedures provide much better agreement between the theoretical spectra and the experimental one

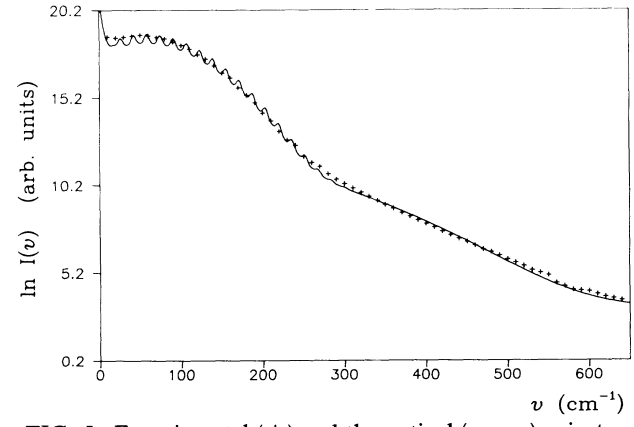

FIG. 5. Experimental (+) and theoretical (——) anisotropic rototranslational spectra of N_2 at 294 K and 170 amagat (Stokes side). In the theoretical spectrum, an exponential contribution $e^{-\nu/\nu_0}$, with ν_0=450 cm^{-1} due to a very-short-range mechanism, has been included.

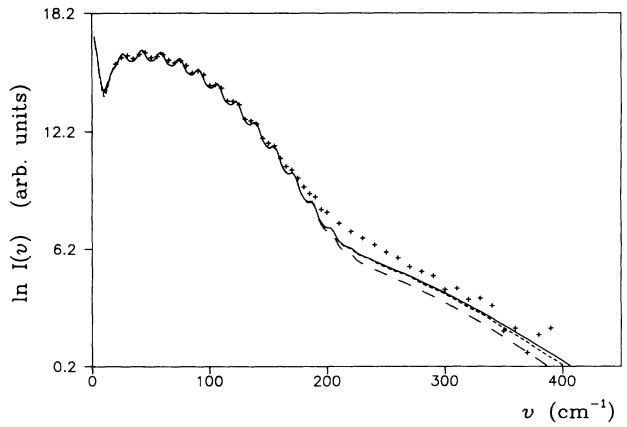

FIG. 6. Experimental (+) and theoretical anisotropic rototranslational spectra of N_2 at 150 K and 40.5 amagat. The theoretical spectra result from the following broadening procedures: (a) (— — —) first order of information theory; (b) (----------) Mori theory; (c) (——) Birnbaum-Cohen theory.

than the theoretical spectrum resulting from information theory.

V. CONCLUSIONS

Anisotropic rototranslational scattering from gaseous nitrogen at the far-frequency range up to about 700 cm^{-1} has been measured at (room) 294 and (low) 150 K temperatures and for densities about 40 and 170 amagat. The experimental spectra have been compared with the theoretical ones obtained from the multipolar light-scattering theory proposed by us, which, for nitrogen, is based on dipole-induced-dipole and dipole-induced-octopole light-scattering mechanisms. We have shown that the DID mechanism alone is not able to describe the far-frequency part of the rototranslational spectra of gaseous N_2. However, if in addition to DID the dipole-induced octopole mechanism is taken into account, agreement between the theoretical and experimental spectra becomes very good. We estimate the absolute value of the dynamic (λ=514.5 nm) irreducible spherical component $\tilde{E}_0^{(4)}$ of the dipole-octopole polarizability tensor as $|\tilde{E}_0^{(4)}|$=4.6 Å^5. Moreover, we found that the far-frequency wings of gaseous nitrogen in the range 300–550 cm^{-1} are almost completely of DIO nature. For the highest-frequency part investigated above 550 cm^{-1}, very short-range interactions are involved. The next multipole contributions (higher order than the octopole) and/or electron overlap are mechanisms suggested for this range of frequency.

ACKNOWLEDGMENTS

We wish to thank Professor Stanisław Kielich for his inspiration of this investigation, and are indebted to Dr. Waldemar Głaz for his great involvement in the early stage of the numerical computations. We wish to thank the University of Angers for their financial support, which made this investigation possible. Moreover, this work has been supported in part by Grant No. 2-0129-91-01 of the Polish Commission for Scientific Studies.

[1] *Intermolecular Spectroscopy and Dynamical Properties of Dense Systems,* Proceedings of the International School of Physics "Enrico Fermi," Course LXXV, Varenna, 1978, edited by J. Van Kranendonk (North-Holland, Amsterdam, 1980).
[2] G. C. Tabisz, *Molecular Spectroscopy* (a Specialist Periodical Report), edited by R. F. Barrow, D. A. Long, and J. Sheridan (Chemical Society, London, 1979), Vol. 6, p. 136.
[3] L. Frommhold, Adv. Chem. Phys., **46**, 1 (1981).
[4] *Phenomena Induced by Molecular Interaction,* edited by G. Birnbaum (Plenum, New York, 1985).
[5] M. A. Proffitt, J. W. Keto, and L. Frommhold, Can. J. Phys. **59**, 1459 (1981).
[6] (a) A. D. Buckingham, and G. C. Tabisz, Opt. Lett. **1**, 220 (1977); (b) Y. Le Duff and A. Gharbi, Phys. Rev. A **17**, 1729 (1978).
[7] A. D. Buckingham and G. C. Tabisz, Mol. Phys. **36**, 583 (1978).
[8] F. Barocchi, A. Guasti, M. Zoppi, S. M. El-Sheikh, G. C. Tabisz, and N. Meinander, Phys. Rev. A **39**, 4537 (1989).
[9] H. Posch, Mol. Phys. **37**, 1059 (1979); **40**, 1137 (1980).
[10] H. Posch, Mol. Phys. **46**, 1213 (1982).
[11] S. Kielich, *Nonlinear Molecular Optics* (Nauka, Moscow, 1981).
[12] (a) G. Maroulis and D. M. Bishop, Mol. Phys. **58**, 273 (1986); (b) I. Cernusak, G. H. F. Diercksen, and A. Sadlej, Chem. Phys. **108**, 45 (1986); (c) P. Isnard, D. Robert, and L. Galatry, Mol. Phys. **31**, 1798 (1976); (d) M. O. Bulanin, in *Spectral Line Shapes,* edited by J. Szudy (Ossolineum, Wrocław, 1989), Vol. 5, p. 597; (e) K. L. C. Hunt, Y. Q. Liang, and S. Sethuraman, J. Chem. Phys. **89**, 7126 (1988).
[13] The trace of the intrinsic polarizability tensor $\vec{a}$ yields a narrow line in the center of the polarized Rayleigh band and is not considered in this work.
[14] B. M. Ladanyi, L. C. Geiger, T. W. Zerda, X. Song, and J. Jonas, J. Chem. Phys. **89**, 660 (1988).
[15] M. S. Brown, Shu-Kun Wang, and L. Frommhold, Phys. Rev. A **40**, 2276 (1989).
[16] A. De Lorenzi, A. De Santis, R. Frattini, and M. Sampoli, Phys. Rev. A **33**, 3900 (1986).
[17] D. Frenkel and J. P. McTague, J. Chem. Phys. **72**, 2801 (1980).
[18] A. De Santis, M. Sampoli, and R. Vallauri, Mol. Phys. **53**, 695 (1985).
[19] P. A. Madden and T. I. Cox, Mol. Phys. **43**, 287 (1981).
[20] F. D. Medina and J. M. Dugas, J. Chem. Phys. **75**, 3252 (1981).
[21] H. Versmold and U. Zimmerman, Mol. Phys. **50**, 65 (1983).
[22] S. Kielich, Proc. Indian Acad. Sci. (Chem. Sci.) **94**, 403 (1985).
[23] T. Bancewicz, W. Głaz, and S. Kielich, Chem. Phys. **128**, 321 (1988).
[24] G. Placzek and E. Teller, Z. Phys. **81**, 209 (1933).
[25] D. A. Varshalovich, A. N. Moskalev, and V. K. Khersonskii, *Kvantovaya Teoria Uglovogo Momenta* (Nauka, Leningrad, 1975).
[26] A. Ben-Reuven and N. D. Gershon, J. Chem. Phys. **51**, 893 (1969).
[27] T. Bancewicz, W. Głaz, and S. Kielich, Phys. Lett. **148**, 78 (1990).
[28] M. Mori, Prog. Theor. Phys. **33**, 423 (1965); **34**, 309 (1965).
[29] G. Birnbaum and E. R. Cohen, Can. J. Phys. **54**, 593 (1976).
[30] C. G. Joslin, C. G. Gray, and Z. Gburski, Mol. Phys. **53**, 203 (1984).
[31] (a) M. S. H. Ling and M. Rigby, Mol. Phys. **54**, 855 (1984); (b) A. van der Avoird, P. E. S. Worner, and A. P. J. Jansen, J. Chem. Phys. **84**, 1629 (1986).
[32] J. O. Hirschfelder, G. F. Curtis, and R. B. Bird, *Molecular Theory of Gases and Liquids* (Wiley, New York, 1954).
[33] A. Raczynski and G. Staszewska, Mol. Phys. **58**, 919 (1986).
[34] W. A. Steele, in *Transport Phenomena in Fluids,* edited by H. H. J. Hanley (Dekker, New York, 1969), Chap. 8.
[35] G. Birnbaum and H. Sutter, Mol. Phys. **42**, 21 (1981).
[36] The scattering plane is that defined by the laser beam and the 90° scattering direction.
[37] B. J. Berne and R. Pecora, *Dynamic Light Scattering* (Wiley, New York, 1976).
[38] L. Frommhold, Can. J. Phys. **59**, 1459 (1981).
[39] V. Teboul, J. L. Godet, and Y. Le Duff, Appl. Spectrosc. (to be published).
[40] A. Michels, R. J. Lunbeck, and G. J. Wolkers, Phys. Grav. **17**, 801 (1951); F. B. CanField, T. W. Lenard and R. Kobayashi, Adv. Cryogen. Eng. **8**, 146 (1963).
[41] G. R. Alms, A. K. Burnham, and W. H. Flygare, J. Chem. Phys. **63**, 3321 (1975).
[42] F. Mulder, G. van Dijk, and A. van der Avoird, Mol. Phys. **39**, 407 (1980).